PCCP

How does the electric current propagate through the fully-hydrogenated borophene?

SCHOLARONE™
Manuscripts

J. Name

ARTICLE

How does the electric current propagate through the fully-hydrogenated borophene?

Yipeng An,*[a,b] Jutao Jiao,[a] Yusheng Hou,[b] Hui Wang,[b] Dapeng Wu,[c] Tianxing Wang,[a] Zhaoming Fu,[a] Guoliang Xu,[a] and Ruqian Wu*[b]

We study the electronic transport properties of two-dimensional (2D) fully-hydrogenated borophene (namely, borophane), using the density functional theory and non-equilibrium Green's function approaches. Borophane shows a perfect electrical transport anisotropy and is promising for applications. Along the peak- or equivalently the valley-parallel direction, the 2D borophane exhibits a metallic characteristic and its current-voltage (*I-V*) curve shows a linear behavior, corresponding to the ON state in borophane-based nano-switch. In this case, electrons mainly propagate *via* the B-B bonds along the linear boron chains. In contrast, the electron transmission is almost forbidden along the perpendicular buckled direction (*i.e.*, the OFF state), due to its semi-conductor property. Our work demonstrates that 2D borophane could combine the metal and semiconductor features and can be a promising candidate of nano-switching materials with stable structure and high ON/OFF ratio.

1 Introduction

Borophene is a new atomically thin two-dimensional nano-sheet and has been successfully synthesized on metallic (*e.g.*, silver) substrates under the ultrahigh-vacuum condition.[1,2] Due to its unique geometric and electronic structures, borophene has attracted broad attention in recent years and many possible exploitations in innovative devices have been proposed.[3-5] For instance, Xiang *et al.*[3] studied the metallic borophene polytypes as lightweight anode materials for non-lithium-ion batteries. Their results provide insights into the configuration-dependent electrode performance of borophene and the corresponding metal-ion storage mechanism. Kistanov *et al.*[4] investigated the routes to localize the carriers and open the band gap of borophene *via* several methods, such as chemical functionalization, ribbon construction, and defect engineering. Jian *et al.*[5] explored the potential of using borophene and defective borophene as anchoring materials for Li-S batteries on the basis of first-principles computations. They found that the defective borophene could be a promising anchoring material and lead to a suppressed shuttle effect and enhanced capacity retention for Li-S batteries.

However, 2D borophene is unstable without suitable substrate based on the theoretical calculations.[6,7] One viable method to stabilize borophene is surface hydrogenation. Xu *et al.*[6] studied the stability of the fully-hydrogenated borophene (borophane) using the first-principles calculation and found that borophane might be stable in vacuum without a substrate. Furthermore, borophane has an ultrahigh Fermi velocity, 4 times higher than that of graphene. Another important feature of borophene is its high mechanical anisotropy along two different directions. Jena *et al.*[7] investigated the possibilities of using borophane as a potential Li and Na-ion
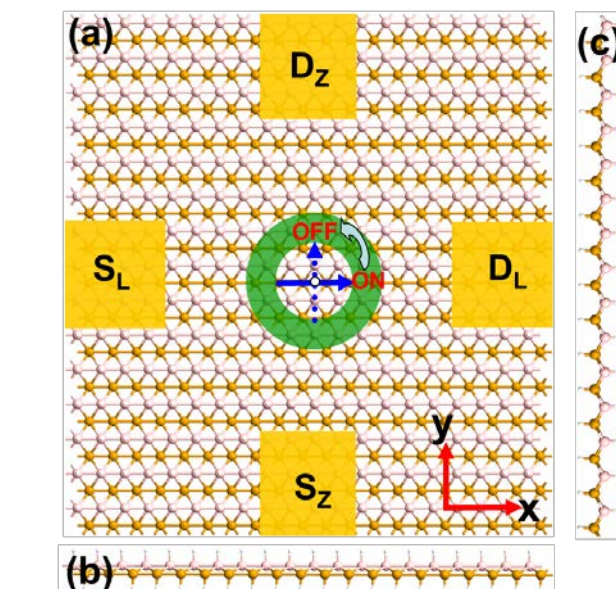

Fig. 1 The nano-switch structure based on the fully-hydrogenated borophene. (a) top, (b) and (c) side views. $S_{L/Z}$ and $D_{L/Z}$ refer to the source and drain electrodes of two-probe system along the x/y direction. The pink/golden color refers to the boron atoms at peak/valley position.

battery anode material through the first-principles calculations. Nevertheless, the electronic and transport properties of borophane have not been carefully examined, which somewhat hindered its applications in nano-electronic devices.
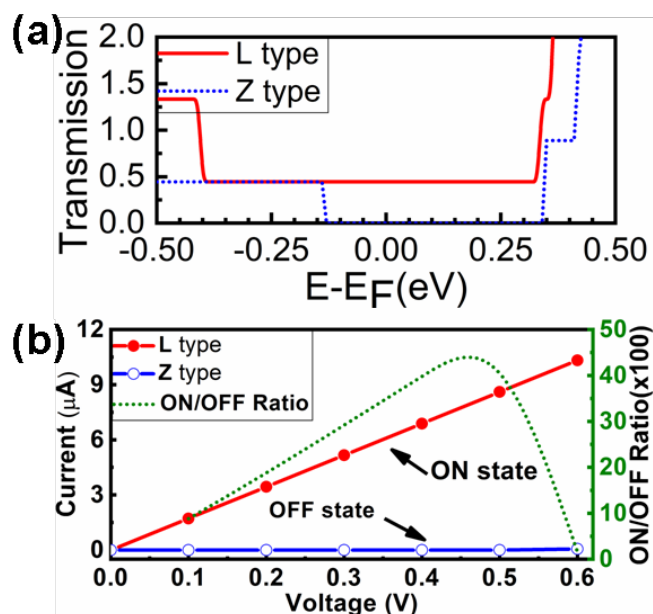
Fig. 2 (a) Transmission spectra of L and Z type borophane two-probe structures under zero bias, (b) their I-V and ON/OFF ratio curves.
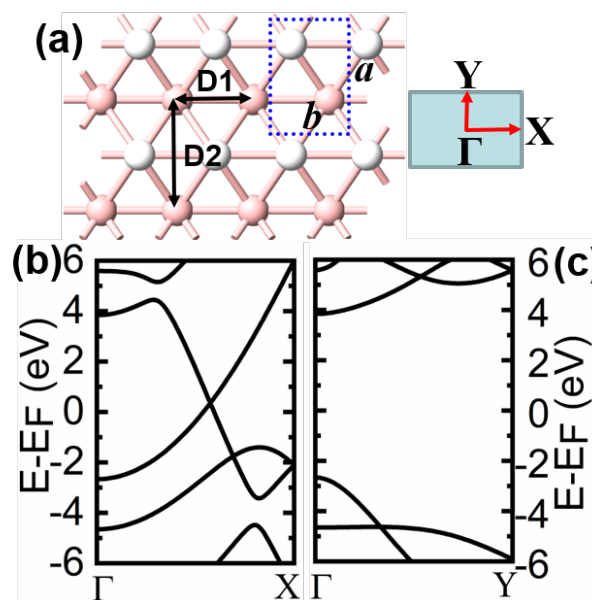

Fig. 3 The super cell (a) and band structures of borophane along x (b) and y (c) directions. The Fermi level is set to zero. D1/D2 refers to the distance between the nearest two boron atoms along the transport direction x/y. The blue dashed box in (a) refers to the unit cell of the borophane, and the first Brillouin zone is shown in the right side.

Borophane has a much better stability than borophene. The main issues regarding its electronic properties are: (1) how strong is its electrical anisotropy? (2) how does the electrical current propagate through the 2D borophane? (3) what unique feature(s) does it have for the use in nano-electronics? To answer these questions, we systematically study the electronic transport properties of borophane (Fig. 1) through density functional theory (DFT) calculations. We find that the 2D borophane has anisotropic current-voltage characteristics along two orthogonal directions, namely, along the x axis (labeled as the L type) and along the y axis (labeled as the Z type), respectively. The *I-V* curve of the L type displays a perfect linear behavior, while it remains zero for the Z type. This suggests that the transports properties of borophane strongly depends on the pattern of hydrogenation and thus can be manipulated for the uses as nano-sensing and nano-switching.

2 Sample structure and method

Figure 1 shows the sample structure of the fully-hydrogenated borophene's two-probe systems, including the top (Fig. 1a) and side views (Figs. 1b and c). We explore its electrical properties along the two orthogonal directions. Namely, one is along the x axis, and the other is along the y axis. In the two-probe structure for each type (L or Z), a 2D supercell is constructed with a periodicity perpendicular to the direction of current between the source ($S_{L/Z}$) and drain ($D_{L/Z}$) electrodes. The third direction (*i.e.*, z axis) is out of the plane, along which the slabs are separated by a 30 Å vacuum. Both $S_{L/Z}$ and $D_{L/Z}$ are semi-infinite in length along the transport direction and are described by a large supercell.

The electronic structures and transport properties are determined by using the first-principles density functional theory and the non-equilibrium Green's function method (*i.e.* NEGF–DFT).[8-11] The GGA-PBE functional is adopted to describe the exchange correlation

interaction among electrons.[12,13] For all boron and hydrogen atoms, their core electrons are described by the optimized norm-conserving Vanderbilt (ONCV) pseudo-potentials, and wave functions of valence states of outer electrons are expanded as linear combinations of atom orbitals (LCAO), based on the level of SG15[14] pseudo-potentials and basis sets. Note that the SG15 datasets of ONCV pseudo-potentials are fully relativistic and provide a good agreement with the all-electron results.[14] For the structural optimization, the residual force on each atom is no more than 10^{-6} eV/Å. We use a $1{\times}9{\times}150$ Monkhorst-Pack k-points grid to sample the Brillouin zone of the left and right electrodes. Note that in the transport direction, the self-energy calculation effectively corresponds to an infinite number of k-points. In this work, we use a 150 k-mesh to achieve a balance between the accuracy and cost, and the electronic structures of the electrodes and central scattering region match well at zero-bias with this selection. Meanwhile, we use 9 k-points in the periodic direction.

3 Results and discussions

Fig. 2a depicts the transmission spectra of the L and Z type two-probe structures of the fully-hydrogenated borophenes. One can see that both of them exhibit the quantization step characteristics, similar to that of graphene or other graphene-like structures.[15-17] Remarkably, the transmission spectrum of the L type exhibits a platform near the Fermi level (E_F), while it is almost zero for the Z type near the E_F. Such remarkable difference should bring about distinct current-voltage behaviors when the bias is applied to the source and drain electrodes.

When a bias V_b is applied, the energies of the source and drain electrodes are shifted accordingly. A positive bias gives rise to an
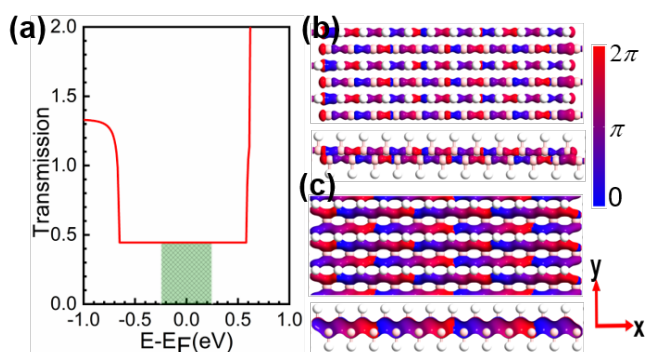
Fig. 4 (a) Transmission spectrum under the bias of 0.5 V, (b) and (c) refer to the two different degenerate transmission eigenstates (TE-I and TE-II) at the Fermi level, including the top and side views. The shadow in (a) refers to the bias window, which contributes to the electric current.

Fig. 5 (a) Top and (b) side views of local transmission pathways of L type two-probe structures at the E_F under the bias of 0.5 V.

electric current from the source to the drain, and vice versa. In the present work, the current I through the L and Z type borophane two-probe systems is obtained by using the Landauer–Büttiker formula[18]

$$I(V_b) = \frac{2e}{h} \int_{-\infty}^{\infty} T(E, V_b)[f_S(E - \mu_S) - f_D(E - \mu_D)]dE, \quad (1)$$

where $T(E, V_b)$ is the bias-dependent transmission coefficient, calculated from the Green's functions, $f_{S/D}$ is the Fermi-Dirac distribution function of the left (L)/right (R) electrode. μ_S (= E_F – $eV_b/2$) and μ_D (= E_F + $eV_b/2$) are the electrochemical potentials of the source and drain electrodes, respectively. More details of the method can be found in previous publications.[10,11]

Fig. 2b gives the *I-V* curves of L and Z type borophane two-probe structures. We can see that they indeed exhibit obvious difference under the limited biases from 0 to 0.6 V. This indicates that borophane has an outstanding electrical anisotropy property, in addition to its mechanical anisotropy property.[6] More explicitly, the *I-V* curve of L type displays a perfect linear behavior like metals. However, the electric current through the Z type is almost zero like semi-conductors or insulators. Based on such *I-V* behaviors of the L and Z type, we propose that the borophane could be used as a nano-switch. That is, the L type is the ON state of the nano-switch, while the Z type corresponds to its OFF state. Then we further calculate its ON/OFF ratio (equals to I_L/I_Z), as shown in Fig. 2b. One can see that such borophane nano-switch has large ON/OFF ratios under the limited biases, and has the peak value at the bias of 0.5 V, which is about 5000 and larger than that of a single-molecule photoswitch (~100).[19]

To understand the large anisotropy of the electronic transport of borophane, we firstly analyze the geometric structure of borophane. The fully-hydrogenated borophene is still out-of-plane buckled and has a similar wrinkle with that of borophene.[1] The blue dashed box in Fig. 3a shows the unit cell of the borophane. We use a 99×99 *k*-points grid for its geometry optimization and band structures calculation. The optimized lattice constants a (= D1) and b (= D2) were determined to be 2.82 and 1.93 Å, agreeing well with previous investigations.[6,20] Along the two different directions, x and y, the
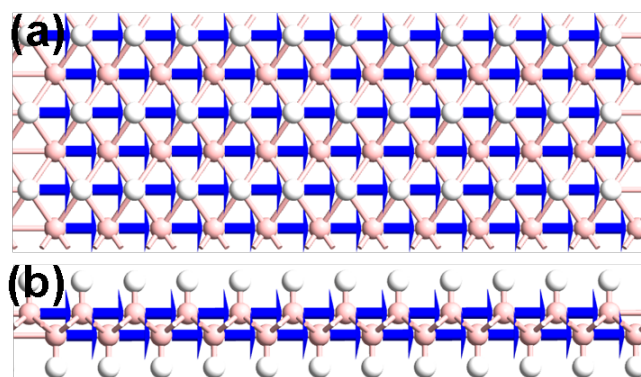
distance (D1/D2) between the nearest boron atoms has obvious difference. As shown in Fig. 3a, for the L type, the D1 (1.93 Å) is far smaller than that (D2) of the Z type, which is about 2.82 Å. Importantly, the nearest boron atoms along the transport direction bind together for the L type, but not for the Z type.

Moreover, the electronic transport properties should depend on their band structures. Namely, electron transmission contains contributions from intra- and inter-band transitions around the Fermi level. To unveil the physical origin of the anisotropy of the electronic transport of borophane, we calculate its band structures along x and y directions, which is located on the *k*-lines from Γ to X (Γ–X) and from Γ to Y (Γ–Y), respectively. It shows completely different band structures along the two *k*-lines Γ–X and Γ–Y (see Figs. 3b and c). One may see that the band structures along Γ–X line (for the L type transport direction) shows a perfect metallic characteristic like that of 2D borophene.[1] However, it presents a semiconductor property with a large direct band gap (~6.5 eV) along Γ–Y line (for the Z type transport direction). All of the results are consistent with previous studies.[6,21] Thus, the anisotropy of the electronic transport of borophane is mostly attributed to the intrinsic difference between its band structures along the x and y directions.

To further disclose the transport channel of borophane at the atomic level, we investigate the transmission spectrum of the L type under the bias of 0.5 V (Fig. 4a) in detail. One can observe that the wide platform is still kept, and the linear electric current is produced near the E_F. There are two different degenerate transmission eigenstates (*i.e.*, TE-I and TE-II) at the E_F, as shown in Figs. 4b and c. Specifically, the TE-I is composed of p_x orbitals of boron atoms, and almost uniformly spread over each boron chain along the x direction. Such continuously uniform distribution is beneficial for electron transmission, and mostly makes the borophane nano-switch open with high mobility. For the TE-II, however, it is disrupted across boron chains and hence the electron transmission along the y axis is effectively blocked.

To give an intuitive understanding on the electron transmission pictures of borophane, we plot the transmission pathways (namely, local currents)[21] of the central scattering region of the L type two-probe structure at the E_F under the bias of 0.5 V (see its top and side views in Figs. 5a and b). The electron transmission pathway is an

analysis option that splits the transmission coefficient into local bond contributions T_{ij}. It has the property that if the system is divided into two parts (A, B), then the pathways across the boundary between A and B sum up to the total transmission coefficient

$$T(E) = \sum_{i \in A, j \in B} T_{ij}(E) \qquad . \qquad (2)$$

Generally speaking, there are two types of local current pathways under a bias. One is *via* chemical bonds (*i.e.*, bond current), and the other is through electron hopping (*i.e.*, hopping current) between atoms which have no strong bonding.[22,23] Our calculated results (see Fig. 5) show that there only exists the bond current for the L type borophane. This bond current locates along the nearest B-B bonds in boron chain, including both the peak and valley positions of the wrinkled fully-hydrogenated borophene. Such linear pathways should have the least barrier and electron scattering for electron transmission. The linear electron transmission pathways are mostly attributed to the TE-I transmission eigenstates, while little contributed by the TE-II transmission eigenstates, as shown in Figs. 4b and c.

4 Conclusions

In conclusion, by using the first-principles density functional theory and the non-equilibrium Green's function method, we investigate the electronic transport properties of the fully-hydrogenated borophene, which still keeps a buckled structure but is more stable. Our results demonstrate that borophane displays a huge electrical anisotropy along with the mechanical anisotropy. Such peculiar electrical anisotropy makes borophane a promising candidate of nano-switches with high ON/OFF ratio. In the peak- and valley-parallel direction (*i.e.*, the L type two-probe structure along the x axis), it shows metallic characteristic and its *I-V* curve is linear. It may keep the circuit conductive, corresponding to the ON state of the borophane-based nano-switch. The p_x orbitals of boron atoms along the x axis mediate the electron transmission through the B-B bonds. Along the buckled direction, in contrast, borophane shows a semiconductor property, corresponding to the OFF state of the borophane-based nano-switch. The giant electrical anisotropy of the 2D fully-hydrogenated borophene is sensitive to the order of H atoms and thus can be useful for nano-sensing.

Acknowledgements

Notes and references

aCollege of Physics and Materials Science & International United Henan Key Laboratory of Boron Chemistry and Advanced Energy Materials, Henan Normal University, Xinxiang 453007, China.
bDepartment of Physics and Astronomy, University of California, Irvine, California 92697-4575, USA
cSchool of Chemistry and Chemical Engineering & International United Henan Key Laboratory of Boron Chemistry and Advanced Energy Materials, Henan Normal University, Xinxiang 453007, China

1   A. J. Mannix, X. F. Zhou, B. Kiraly, J. D. Wood, D. Alducin, B. D. Myers, X. L. Liu, B. L. Fisher, U. Santiago, J. R. Guest, M. J. Yacaman, A. Ponce, A. R. Oganov, M. C. Hersam and N. P. Guisinger, *Science*, 2015, **350**, 1513–1516.

2   B. J. Feng, J. Zhang, Q. Zhong, W. B. Li, S. Li, H. Li, P. Cheng, S. Meng, L. Chen and K. H. Wu, *Nature Chem.*, 2016, **8**, 563–568.

3   P. Xiang, X. F. Chen, W. T. Zhang, J. F. Li, B. B. Xiao, L. S. Li and K. S. Deng, *Phys. Chem. C hem. Phys.*, 2017, **19**, 24945–24954.

4   A. A. Kistanov, Y. Q. Cai, K. Zhou, N. Srikanth, S. V. Dmitriev and Y. W. Zhang, *Nanoscale*, 2018, **10**, 1403–1410.

5   H. R. Jiang, W. Shyy, M. Liu, Y. X. Ren and T. S. Zhao, *J. Mat er . Chem. A*, 2018, **6**, 2107–2114.

6   L. C. Xu, A. J. Du and L. Z. Kou, *Phys. Chem. Chem. Phys.*, 2016, **18**, 27284–27289.

7   N. K. Jena, R. B. Araujo, V. Shukla and R. Ahuja, *ACS Appl. Mater. Interfaces*, 2017, **9**, 16148−16158.

8   ATK, http://quantumwise.com/.

9   J. M. Soler , E. Artacho E, J. D.Gale , A. García, J. Junquera, P. Ordejón and D. Sánchez-Portal, *J. Phys: Condens Matter.*, 2002, **14**, 2745−2779.

10   M. Brandbyge, J. L. Mozos, P. Ordejón, J. Taylor and K. Stokbro, *Phys. Rev. B*, 2002, **65**, 165401.

11   J. Taylor, H. Guo and J. Wang, *Phys. Rev. B*, 2001, **63**, 121104.

12   J. P. Perdew, J. A. Chevary, S. H. Vosko, K. A. Jackson, M. R. Pederson, D. J. Singh and C. Fiolhais, *Phys. Rev. B*, 1992, **46**, 6671.

13   J. P. Perdew, K. Burke and M. Ernzerhof, *Phys. Rev. Lett.*, 1996, **77**, 3865.

14   M. Schlipf and F. Gygi, *Comput. Phys. Commun.*, 2015, **196**, 36−44.

15   Z. Y. Li, H. Y. Qian, J. Wu, B. L. Gu and W. H. Duan, *Phys. Rev. Lett.*, 2008, **100**, 206802.

16   Y. P. An, M. J. Zhang, L. P. Chen, C. X. Xia, T. X. Wang, Z. M. Fu, Z. Y. Jiao and G. L. Xu, *RSC Adv.*, 2015, **5**, 107136–107141.

17   M. J. Zhang, Y. P. An, Y. Q. Sun, D. P. Wu, X. N. Chen, T. X. Wang, G. L. Xu and K. Wang, 2017, **19**, 17210–17215.

18   M. Büttiker, Y. Imry, R. Landauer and S. Pinhas, *Phys. Rev. B*, 1985, **31**, 6207−6215.

19   C. Jia, A. Migliore, N. Xin, S. Huang, J. Wang, Q. Yang, S. Wang, H. Chen, D. Wang, B. Feng, Z. Liu, G. Zhang, D. H. Qu, H. Tian, M. A. Ratner, H. Q. Xu, A. Nitzan and X. Guo,

Science, 2016, **17**, 1443−1445.

20   T. Cheng, H. F. Lang, Z. Z. Li, Z. F. Liu and Z. R. Liu, *Phys. Chem. Chem. Phys.*, 2017, **19**, 23942–23950.

21   G. C. Solomon, C. Herrmann, T. Hansen, V. Mujica and M.A. Ratner, *Nat. Chem.*, 2010, **2**, 223−228.

22   A. H. CastroNeto, F. Guinea, N. M. R. Peres, K. S. Novoselov and A. K. Geim, *Rev. Mod. Phys.*, 2009, **81**, 109–162.

23   L. Shen, M. G. Zeng, S. C. Li, M. B. Sullivan and Y. P. Feng, *Phys. Rev. B*, 2012, **86**, 115419.